Received: 8 March 2022 | Revised: 6 September 2022 | Accepted: 7 September 2022

DOI: 10.1111/joa.13770

Journal of Anatomy ANATOMICAL SOCIETY WILEY

ORIGINAL ARTICLE

Re-description of the early Triassic diapsid *Palacrodon* from the lower Fremouw formation of Antarctica

Kelsey M. Jenkins[1,2] | Dalton L. Meyer[1] | Patrick J. Lewis[3] | Jonah N. Choiniere[4] | Bhart-Anjan S. Bhullar[1,2]

[1]Department of Earth and Planetary Sciences, Yale University, New Haven, Connecticut, USA

[2]Peabody Museum of Natural History, Yale University, New Haven, Connecticut, USA

[3]Department of Biological Sciences, Sam Houston State University, Huntsville, Texas, USA

[4]Evolutionary Studies Institute, University of the Witwatersrand, Johannesburg, South Africa

Correspondence
Kelsey M. Jenkins and Bhart-Anjan S. Bhullar, Department of Earth and Planetary Sciences, Yale University, New Haven, CT, USA.
Email: kelsey.jenkins@yale.edu; bhart-anjan.bhullar@yale.edu

Funding information
Department of Earth and Planetary Sciences, Yale University; Sigma Xi; NRF African Origins Platform, Grant/Award Number: 98800; National Science Foundation, Grant/Award Number: 2046868

Abstract

The rapid radiation and dispersal of crown reptiles following the end-Permian mass extinction characterizes the earliest phase of the Mesozoic. Phylogenetically, this early radiation is difficult to interpret, with polytomies near the crown node, long ghost lineages, and enigmatic origins for crown group clades. Better understanding of poorly known taxa from this time can aid in our understanding of this radiation and Permo-Triassic ecology. Here, we describe an Early Triassic specimen of the diapsid *Palacrodon* from the Fremouw Formation of Antarctica. While *Palacrodon* is known throughout the Triassic and exhibits a cosmopolitan geographic range, little is known of its evolutionary relationships. We recover *Palacrodon* outside of crown reptiles (Sauria) but more crownward than *Youngina capensis* and other late Permian diapsids. Furthermore, *Palacrodon* possesses anatomical features that add clarity to the evolution of the stapes within the reptilian lineage, as well as incipient adaptations for arboreality and herbivory during the earliest phases of the Permo–Triassic recovery.

KEYWORDS
arboreal, evolution, fossil, mass extinction, paleontology, Permian, reptile, stapes

1 | INTRODUCTION

Reptiles rapidly diversified following the end-Permian mass extinction, evolving disparate body plans (Botha & Smith, 2006; Ezcurra & Butler, 2018). However, the early evolution of reptilian subclades is obscured by this rapid radiation in the wake of the biotic crisis. Our understanding of early reptilian diversification is further hampered by sampling bias—fossiliferous continental deposits close to the PT boundary are rare (Romano et al., 2020). As a result, the origins of many distinctive, specialized taxa that appear in the latter portions of the Triassic are enigmatic, and the acquisition of important adaptations (e.g., impedance matching ears) are inscrutable. Transitional forms from this time have excellent potential to shed light on reptilian phylogeny and provide information on the homology and origins of key adaptations that enabled reptiles to dominate the Mesozoic, and arguably today.

The Lower Triassic Fremouw Formation of Antarctica is one of the few fossiliferous terrestrial localities that straddles the Permo-Triassic boundary (McManus et al., 2002; Peecook et al., 2018). Historical excavations there have yielded numerous tetrapods, including temnospondyls, cynodonts, stem and crown reptiles, and the enigmatic reptile genus *Palacrodon* (Romano et al., 2020), which was collected in 1969 from Kitching Ridge, an Early Triassic exposure of the Fremouw Formation (Kitching et al., 1972). *Palacrodon* has a varied phylogenetic history in which it has been dubbed a rhynchocephalian, "lizard," procolophonid, and trilophosaurid, though currently stands as Diapsida *incertae sedis* (Gow, 1992, 1999; Kligman et al., 2018; taxonomic history further summarized in Figure S1). *Palacrodon* has the potential to fill some of these gaps in Permo-Triassic reptile evolution, but it remains mostly known from isolated cranial fragments containing teeth that provide few phylogenetically informative characters. Because of this, *Palacrodon* was distinctly omitted from the earliest phylogenetic

analyses of reptiles (Gauthier et al., 1988), and its phylogenetic position has not been considered in more recent studies. Despite this, *Palacrodon* is an important biostratigraphic marker for the South African *Cynognathus* Assemblage Zone (Hancox et al., 2020), and its 35-million-year stratigraphic range spanning both hemispheres (Kligman et al., 2018) makes it an important global index taxon that biostratigraphically links the northern and southern continents. Still, *Palacrodon* as well as many other taxa from this time are undersampled and understudied (Pusch et al., 2021), highlighting the gaps in our understanding of Triassic ecology.

Here we use CT scans to reexamine the most complete specimen of *Palacrodon* Gow 1906 (BP/1/5296, Evolutionary Studies Institute, University of the Witwatersrand, Johannesburg, South Africa), which preserves portions of the skull in articulation and postcranial elements that were never described before. Our revised description of *Palacrodon* provides new insights into the morphology of this taxon, allowing us to place it within a quantitative phylogenetic analysis for the first time.

2 | METHODS

2.1 | CT scanning and segmentation

The specimen is a partial, mostly disarticulated skeleton (BP/1/5296). The specimen was scanned at the Evolutionary Studies Institute at the University of the Witwatersrand in Johannesburg, South Africa, using a Nikon Metrology micro-CT scanner with a resolution of 22.5 μm and produced a stack of 1161 tomographs. The stack was imported into VGStudio Max version 3.0 where the fossil was digitally segmented from the surrounding matrix using the region growing tool. 3D renderings were created using the Scatter HQ setting, while slice images are shown as is. Raw μCT scan data as well as 3D meshes of segmented bones have been uploaded to Morphosource.org.

2.2 | Phylogenetic analyses

We investigated the phylogenetic position of *Palacrodon* in both parsimony and Bayesian frameworks using all available material of BP/1/5296 and its published latex peel and photograph. Other South African and North American material for this genus was not considered for character scoring as we question the intergeneric relationships of various specimens. We used a previously published matrix consisting of 337 morphological characters and 62 taxa including early diapsid and crown reptiles, including *Palacrodon* (Pritchard & Sues, 2019). Two modifications were made to the characters within this matrix: (1) we added an additional character state to Character 118 to capture the intermediate shape of the stapes in *Palacrodon* and other near-crown stem-reptiles, and (2) Character 338 was added to capture the ratio of the posterior portion of the skull to that of the orbit, inferred from the outline of the skull seen in the published photograph of the latex peel that shows portions of the skull in situ. More detailed information on these characters can be found in the Supplement. *Colobops noviportensis* was also removed from the taxon list of this matrix due to the conflicting placement of this taxon within Archosauromorpha (Pritchard et al., 2018) or Lepidosauromorpha (Scheyer et al., 2020).

Parsimony analyses were conducted in TNT version 1.5 (Goloboff & Catalano, 2016), with *Petrolacosaurus kansensis* selected as the outgroup (Figure S2–S5). For equal weights analyses, driven searches were performed using the new technology search function starting with 50 random addition sequences and searching for the minimum length 100 times. Sectorial searching, ratchet, drift, and tree fusing were all active and default settings for all were used with the exception of extending the ratchet to 100 total iterations. The resultant trees in the RAM were then subjected to a round of traditional search by TBR to further explore tree islands. For all parsimony analyses, characters were ordered as indicated within the Supplement.

Parsimony analyses were performed using implied weights (K = 12), because it has been suggested to outperform other methods of phylogenetic inference for morphological data (Goloboff et al., 2018). The implied weight analyses were conducted in the same fashion as the equal weights parsimony analyses, with the exception of using the default settings for reaching a stabilizing consensus. As an additional measure of sensitivity, we performed weighted analyses for K values of 3 and 6. Without implied weighting, branch supports were calculated with a bootstrap analysis using frequency differences ("GC") and absolute frequencies of 1000 pseudoreplicates utilizing a traditional (heuristic) search with 1000 Wagner trees holding 100 trees per replicate. Implied weighting bootstrap supports were calculated with a new technology search (sectorial search, ratchet, drift, tree fusing) of 1000 pseudoreplicates with 10 random additional sequences and finding a minimum length one time. Additional supports for all analyses were calculated through symmetric resampling (GC) with a 33% change probability using a new technology search (sectorial search, ratchet, drift, tree fusing) with 10 random additional sequences and finding a minimum length one time.

An unconstrained Bayesian analysis was also conducted using the Mkv model of morphological character state evolution in the program MrBayes version 3.2.7 (Figure S6; Huelsenbeck & Ronquist, 2001), with Lewis correction for using parsimony-informative characters (Lewis, 2001). Ten million generations were requested, and the analysis terminated once average deviation of split frequencies dropped below 0.01. Convergence was achieved after <10,000,000 generations and was checked using the output garnered from the sump command in MrBayes. The resulting phylogeny was then imported into FigTree version 1.4.4 to reroot *Petrolacosaurus kansensis* as the outgroup taxon.

3 | SYSTEMATIC PALEONTOLOGY

Reptilia Laurenti, 1768.
Diapsida Osborn, 1903.
Type genus: *Palacrodon* Broom, 1906.

Generic diagnosis

The presence of labiolingually expanded crowns, often described as molariform, that are ankylosed to the apex of the bone (i.e., acrodont). The basal portion of the crown is often bulbous, and labial and lingual surfaces protrude past their respective margins of the jawbone, and in some specimens, appear fused to one another. Teeth are triangular in lateral view and there is no evidence of replacement. Unworn crowns bear two to three labiolingually oriented cusps on their occlusal surface attached by a ridge.

Constituent species: *Palacrodon browni*, *Palacrodon sp.*

Known distribution

Specimens of the genus *Palacrodon* are known from the Early Triassic of Antarctica (Gow, 1992), the Early to Middle Triassic of South Africa (Broom, 1906; Gow, 1999; Neveling, 2004), and the Late Triassic of Arizona (Kligman et al., 2018).

Type species

Palacrodon browni, SAM-PK-5871, partial left lower jaw containing six teeth, Iziko South African Museum, Cape Town, South Africa. The holotype was collected by Alfred "Gogga" Brown from an unknown South African locality, likely near Aliwal North (Broom, 1906).

Remarks

The specimen examined herein was originally described as the diapsid *Fremouwsaurus geludens* before it was synonymized with *Palacrodon* (Gow, 1992, 1999). BP/1/5296 represents the stratigraphically

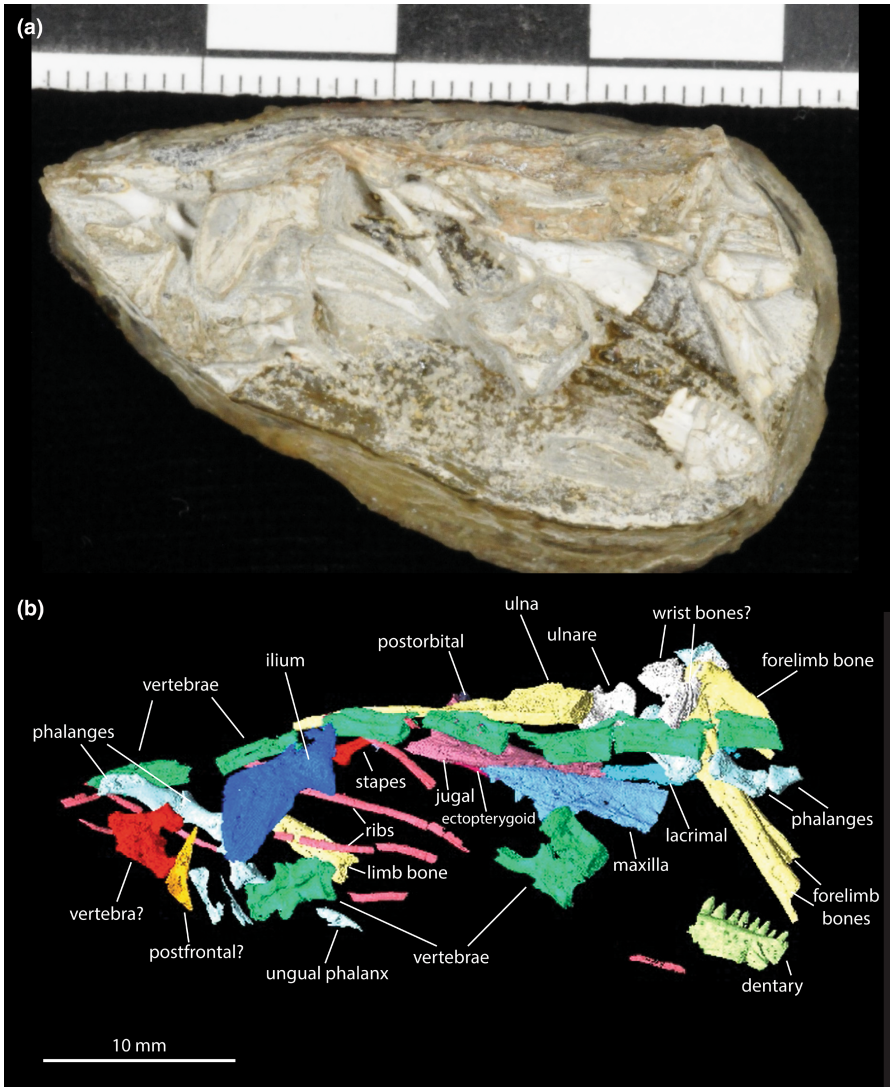

FIGURE 1 BP/1/5296 *Palacrodon* sp. from the lower Fremouw formation of Antarctica. (a) Specimen in its current form; (b) CT scanned material in situ.

lowest instance of this taxon, but the precise stratigraphic position of BP/1/5296 is unknown. Other taxa collected from Kitching Ridge (*Lystrosaurus*, *Procolophon*, *Prolacerta*) suggest it was collected from a lower member of the Fremouw Formation and is approximately Induan in age (Collinson et al., 2006; Sidor et al., 2008; Smith et al., 2011). The faunal composition of the lower Fremouw formation is similar to that of the *Lystrosaurus* Assemblage Zone of South Africa, though some taxa such as *Palacrodon* are only found in the *Cynognathus* Assemblage Zone (Hancox et al., 2020).

BP/1/5296 is the most complete specimen of *Palacrodon* (Figure 1), and it is described herein. This specimen has been referred to as *Palacrodon broomi* in recent publications (Smith et al., 2011; Spiekman, 2018), but that epithet is likely a misquoting of the only established species name *Palacrodon browni*. The apomorphic dentition present in South African and North American specimens link BP/1/5296 to the genus *Palacrodon*, but because other comparative material is lacking, we cannot refer to this specimen as *Palacrodon browni* and do not assign it a species name.

3.1 | Osteology of *Palacrodon* sp. (BP/1/5296)

BP/1/5296 was originally described using a latex peel created from an impression of the original material in the matrix (Gow, 1992). Since that description, the specimen was prepared within a resin backing (Figure 1A), obscuring many of the details originally described, though some impression of the maxilla and dentary, including dentition, are still visible. The latex peel that is the basis of the original description is also lost and cannot be referenced other than the photograph figured in the earlier publication. The latex peel revealed the shapes of some unpreserved elements visible in negative relief and the CT scan revealed portions of the specimen that were formerly embedded in the matrix.

3.2 | Cranial skeleton

The right maxilla, jugal, lacrimal, postorbital, and ectopterygoid are the only well-articulated cranial elements (Figure 2), while the left postfrontal, right stapes, a fragment of the right quadrate, and the anterior portion of the dentary and splenial are not articulated with other elements of the skull. However, the articulated cranial bones and at least the dentary are thought to be preserved in situ because impressions of the missing portions of the maxilla and dentary reveal where these bones would have articulated.

3.2.1 | Maxilla

The posterior end of the right maxilla is preserved in articulation with the jugal and lacrimal and measures 9.25 mm anteroposteriorly

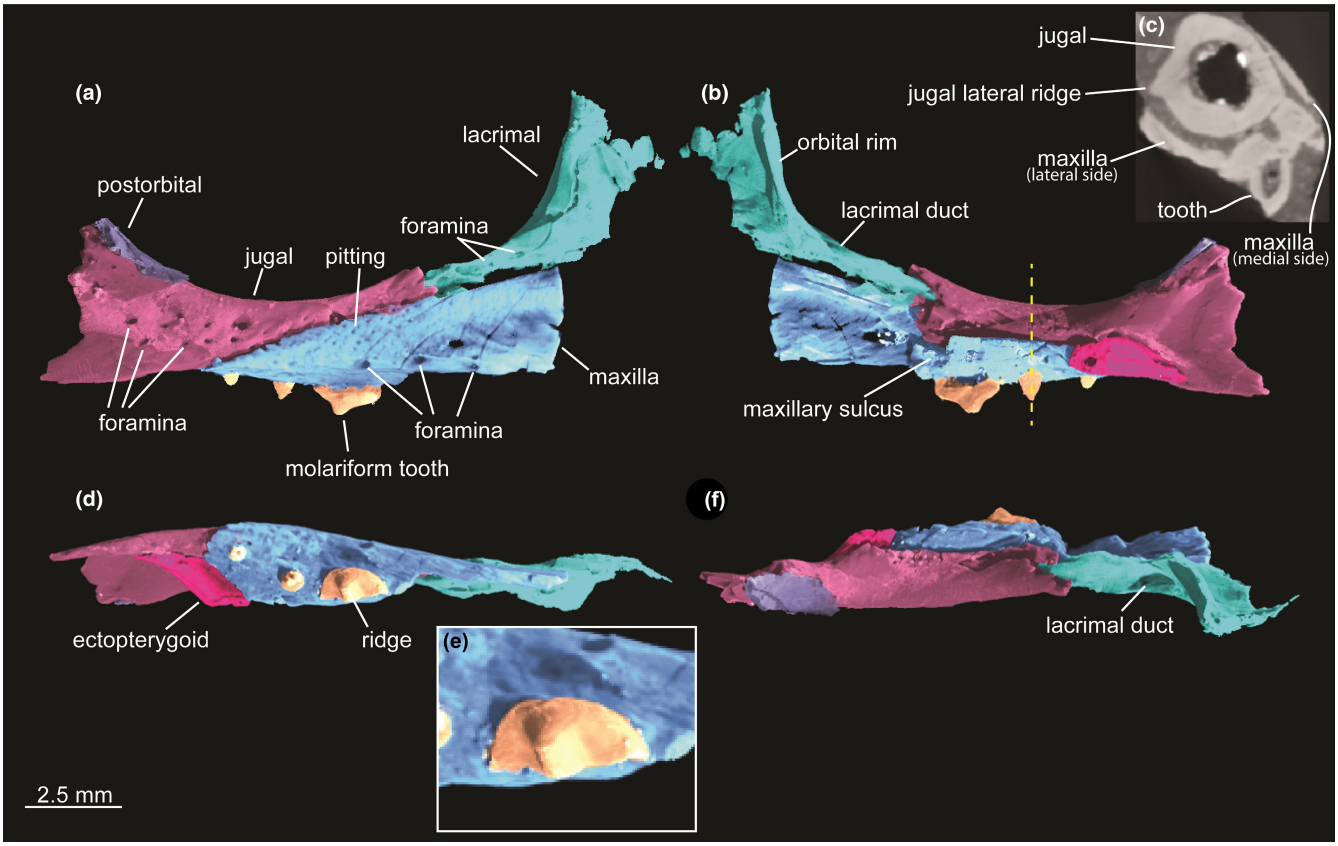

FIGURE 2 Articulated bones of the ventral portion of the right orbital margin from BP/1/5296. (a) Lateral view, (b) medial view, (c) coronal slice as indicated by the dotted line in (b, d) ventral view, (e) close-up view of molariform tooth in (d, and f) dorsal view.

(Figure 2). The lateral surface at its tallest measures 2.8 mm and tapers posteriorly. It bears two foramina, the posteriormost of which lies above a partially preserved molariform tooth. Fine pitting is present on the lateral surface directly dorsal to these foramina that is not present on any of the adjacent bones. The medial portion of the maxilla is only preserved dorsal to the teeth. The maxilla bears a longitudinal sulcus dorsally, which wraps around the ventral surface of the anterior process of the jugal. The ventral surface bears three teeth that exhibit acrodont implantation, which are ankylosed to the adjacent bone. The anteriormost tooth is only partially preserved but exhibits the apomorphic molariform shape associated with the genus *Palacrodon*; this includes an expanded tooth base relative to the apex, and an apical ridge that runs labiolingually. Its mesiodistal length measures 1.7 mm. The molariform tooth is succeeded by two small, conical teeth that respectively measure 0.53 and 0.39 mm in diameter. Posteromedially, the maxilla contacts the ectopterygoid, and this contact is visible in ventral and medial views.

3.2.2 | Jugal

The right jugal is approximately triangular in lateral and medial view and it forms nearly the entire ventral edge of the orbit (Figure 2). Anteriorly it meets the posterior process of the lacrimal, excluding the maxilla from the orbital margin. Its lateral surface bears a prominent ridge that extends anteroposteriorly along the surface of the anterior process where it is received by the maxilla (Figure 2c & 3). The anterior process is approximately 3 mm in diameter. The lateral surface bears two parallel rows of foramina, orientated in the horizontal plane. The dorsal row comprises five foramina, while the ventral row comprises four. Unlike what was previously described (Gow, 1992), the jugal does not possess a backwards projecting jugal spur (i.e., posterior process); this misidentification is likely a result of the broken posterior lamina. Due to the breakage, it cannot be determined if the jugal was a fully triradiate element indicative of well-developed temporal fenestration like what is seen in *Youngina capensis* (Figure 3e,f), or if the posterior process of the jugal was broader in shape such as that of more basal taxa (Figure 3a,b). The anterior surface of the dorsal lamina bears a facet that receives the ventral margin of the postorbital. Its maximum anteroposterior length is 9.45 mm.

3.2.3 | Lacrimal

The right lacrimal is poorly preserved and the interpretable portion is limited to the orbital margin. The lateral surface is smooth,

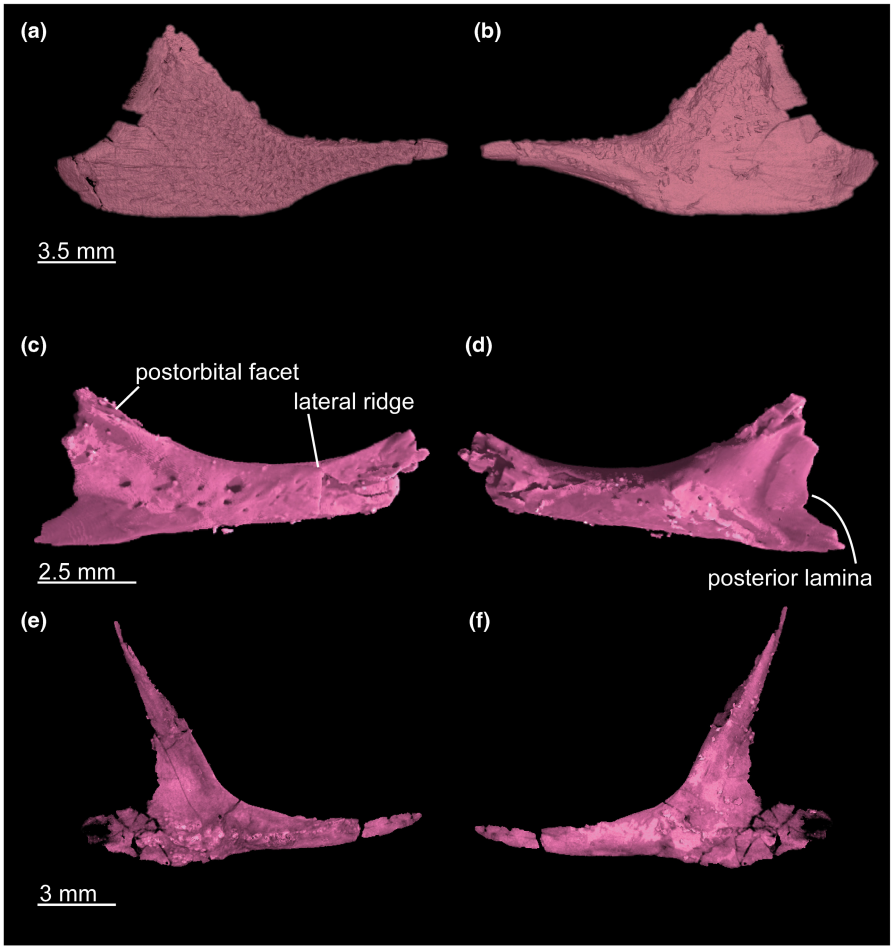

FIGURE 3 Jugals of stem reptiles. Right jugal of *Euconcordia cunninghami* (KUVP 87102, The University of Kansas, Lawrence, Kansas, United States) in (a) lateral and (b) medial view; right jugal of *Palacrodon* sp. in (c) lateral and (d) medial view; right jugal of *Youngina capensis* (BP/1/375) in (e) lateral and (f) medial view.

other than two minor foramina present on the posterior process. The medial surface is reinforced by an orbital rim that runs dorsoventrally, creating the posterior border of the nasal capsule. The lacrimal duct is mildly exposed in medial view, though is well-exposed when viewed dorsally. The ventral margin of the lacrimal contacts the maxilla, though this contact is somewhat degraded, preventing confident assessment of the nature of contact between the two bones.

3.2.4 | Postorbital

Only a small fragment of the ventral portion of the right postorbital is present, but it is identifiable due to its articulation with the jugal posteroventrally. What is preserved of this bone composes the posteroventral portion of the orbital margin. No foramina, pitting, or other identifying marks are present.

3.2.5 | Ectopterygoid

The portion of the right ectopterygoid that is preserved contacts both the jugal and the maxilla. However, the portion of the ectopterygoid that would contact the other bones of the palate, namely the pterygoid and perhaps the palatine, is not preserved. It cannot be determined if an additional facet on the maxilla existed for the reception of the anterolateral process of the ectopterygoid, if it existed.

3.2.6 | Postfrontal

An isolated left postfrontal is present (Figure 4a–d). The lateral portion of the bone is curved, indicating that it formed a portion of the orbital rim. The medial portion is flat and likely bordered a midline element, likely the frontal. It cannot be determined if the postfrontal participated in the upper temporal fenestra.

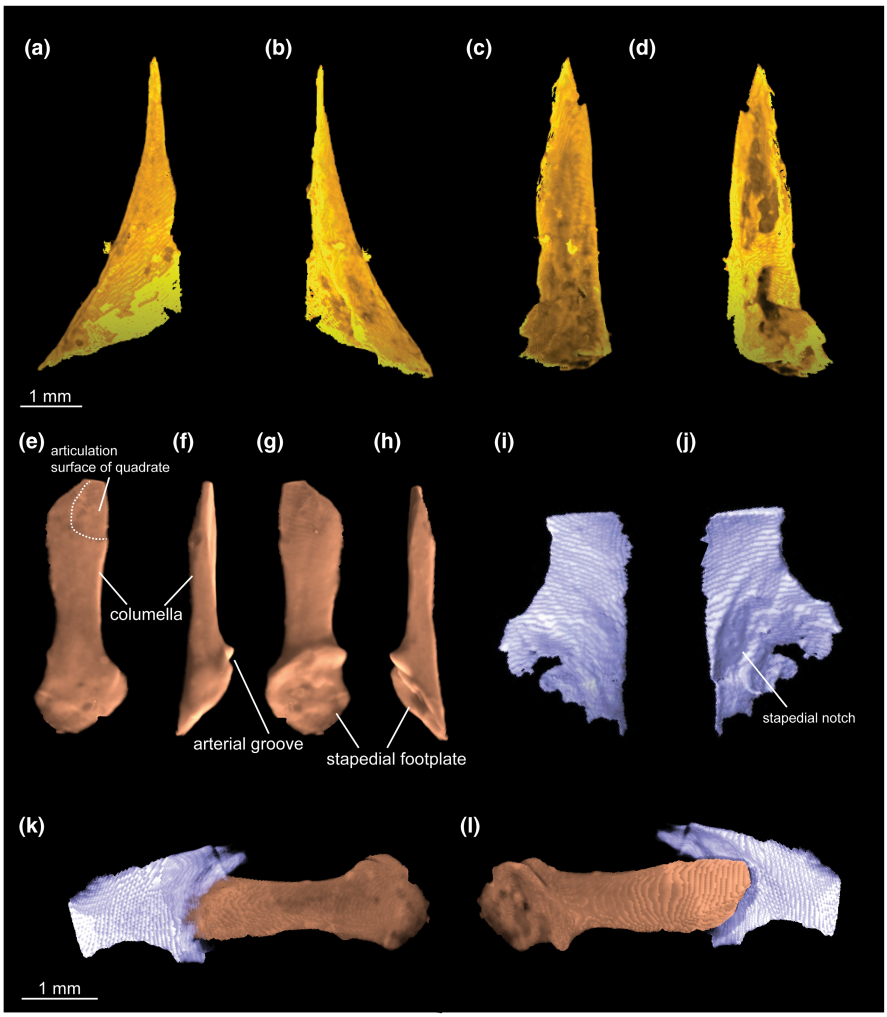

FIGURE 4 Postfrontal, stapes, and quadrate from BP/1/5296. Left postfrontal in (a) dorsal, (b) ventral, (c) lateral, and (d) medial views; right stapes in (e) anterior, (f) dorsal, (g) posterior, (h) and ventral views; fragmented right quadrate in (i) lateral and (j) medial views; stapes and quadrate in situ in (k) lateral and (l) medial views.

3.2.7 | Stapes

A right stapes (previously identified as an epipterygoid [Gow, 1992]) is present and semi-articulated with a partial quadrate (Figure 4e–h,k,l). The columella is broad dorsoventrally but much narrower anteroposteriorly, and its maximum length measures 3.30 mm. The stapes is much broader than those of other near-crown stem reptiles (Gardner et al., 2010), but not nearly as robust as the condition of earlier-branching forms such as *Captorhinus laticeps* (Heaton, 1979), *Australothyris smithi* (Modesto et al., 2009), and *Orovenator mayorum* (Ford & Benson, 2019). The articular surface of the stapes for the quadrate is present, but is not a prominent feature. No stapedial foramen is present, but an arterial groove is visible at the occipital margin of the stapedial footplate.

3.2.8 | Quadrate

Only a small portion of a partial right quadrate (Figure 4i–l; previously identified as a squamosal [Gow, 1992]) is identified, contrary to what is figured in the original description. The original description illustrated a larger portion of the right quadrate, including its articular surface, visible in lateral profile from the impression of the latex peel. However, the specimen in its current state does not preserve impressions of a larger portion of the quadrate. The preserved portion possesses little identifiable anatomy, other than the stapedial notch located on the medial side.

3.2.9 | Dentary

The anterior portion of a right dentary is preserved (Figure 5). Eight teeth are present, aligned in a single tooth row and increase in height as they progress posteriorly. The first six teeth are somewhat slender and conical, while the last two are more bulbous and possess a tapering apex. No ridges or serrations are present on the teeth. Tooth implantation appears acrodont and teeth are ankylosed to the adjacent bone (Figure 5d,e). The anteriormost two teeth of the tooth row are procumbent, while the rest of the teeth are aligned more or less vertically. Eight large foramina are aligned horizontally along the lateral surface of the dentary. The medial portion of the dentary is poorly preserved, but the anterior dentary symphysis is visible. The symphysis is oriented dorsoventrally and does not possess any distinct curvature. What is visible of the Meckelian canal is subcircular in coronal sliced view and excavates the internal dorsal surface of the splenial (Figure 5d), however, it is degraded in the more anterior portion of the lower jaw (Figure 5e).

3.2.10 | Splenial

The anterior portion of the splenial is preserved on the medial side of the dentary (Figure 5b). Medially, a large foramen intermandibularis is present, located ventrally beneath the sixth tooth; it is fully contained by the splenial. The anterior end does not participate in the jaw symphysis.

3.3 | Postcranial skeleton

3.3.1 | Vertebrae

Two disarticulated dorsal vertebrae are preserved along with portions of eight semi-articulated caudal vertebrae (Figure 6). Potentially another neural arch is preserved (Figure 1a, "vertebra?") but it is

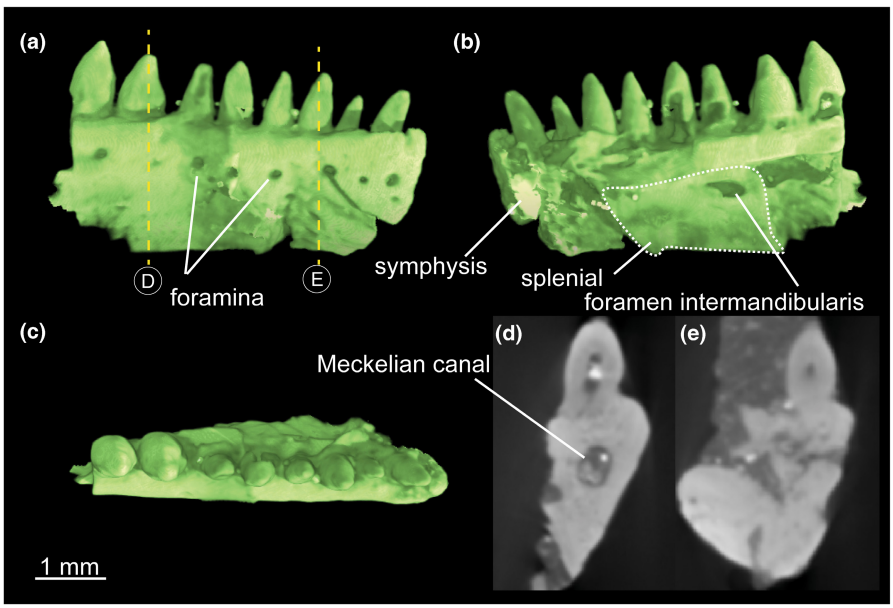

FIGURE 5 Lower jaw from BP/1/5296. Right dentary in (a) lateral view, (b) medial view, with splenial indicated by white dotted outline, (c) dorsal view, (d, e) slice views as indicated by the dotted lines in a.

compressed dorsoventrally, distorting the interpretation of this bone. While the two dorsal vertebrae do not appear compressed, the neural arches are somewhat distorted as they are tilted laterally. The articulating surfaces of all centra are flat, indicating acoelous vertebral articulation, and vertebrae are not notochordal. No traces of intercentra or haemal arches are present.

Of the two dorsal vertebrae, one is represented only by the neural arch (Figure 6p–u). The two vertebrae likely occupied a proximal position to one another if they did not directly articulate. While they are not articulated, the neural arches are similar in morphology and size (Table 1). Laterally both the transverse processes are partially preserved on the right and left sides, and the neural spine is better developed. It preserves an anteroventrally-to-posterodorsally inclined transverse process. The latter vertebra (Figure 6j–o) also preserves an anteroventrally-to-posterodorsally inclined transverse process on the right lateral side, though it is more steeply inclined. This inclination of

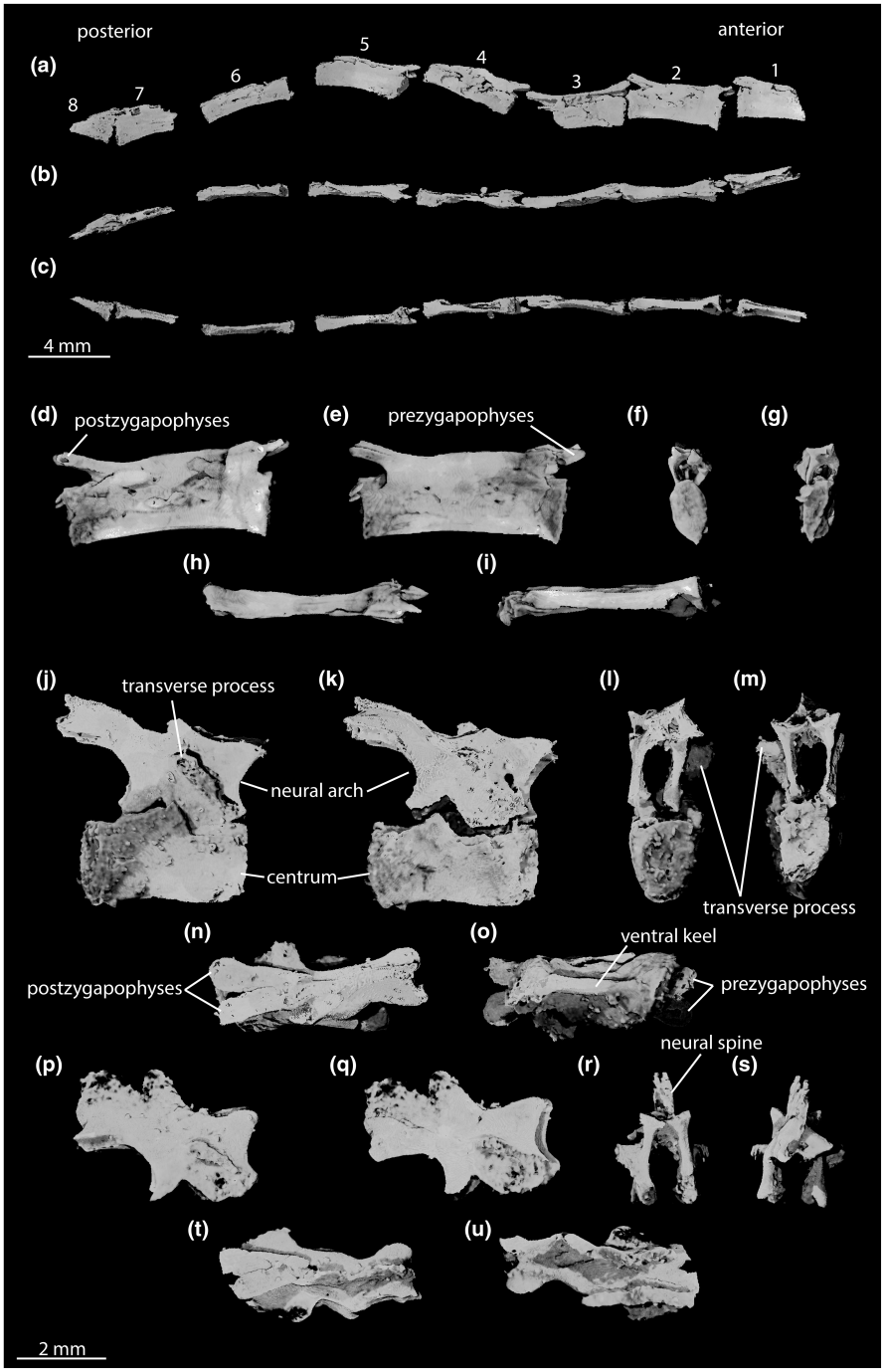

FIGURE 6 Vertebrae from BP/1/5296. Eight partial or complete semi-articulated caudal vertebrae in (a) right lateral, (b) dorsal, and (c) ventral view. (d–i) vertebrae 2 from (a–c) in (d) right lateral, (e) left lateral, (f) anterior, (g) posterior, (h) dorsal, and (i) ventral view. Single dorsal vertebra in (j) right lateral, (k) left lateral, (l) anterior, (m) posterior, (n) dorsal, and (o) ventral view. Neural arch from dorsal vertebra in (p) right lateral, (q) left lateral, (r) anterior, (s) posterior, (t) dorsal, and (u) ventral view.

TABLE 1 Dorsal vertebrae measurements from BP/1/5296 as they appear in Figure 6. Measurements reported in millimeters.

Vertebra	Anteroposterior length of centrum	Centrum height	Centrum width	Neural arch height	Neural arch width	Total height
Figure 6d–i	4.48	1.42	0.74	0.64	0.91	2.06
Figure 6j–o	3.70	1.78	1.46	2.68	1.80	4.46
Figure 6p–u	–	–	–	2.90	2.05	–

the transverse process is similar to what is seen in the anterior dorsal vertebrae of *Youngina capensis* (Gow, 1975) and the mid-to-posterior dorsal vertebrae of *Thadeosaurus colcanapi* (Carroll, 1981). Well-developed, horizontally inclined zygopophyses are visible dorsally, and aside from a ventral keel, no distinct features are present on the ventral surface. Interestingly, the neural arch is quite tall, best visible anteriorly and posteriorly, and is taller than the height of the centrum (Table 1).

The series of eight caudal vertebrae are laterally compressed, and would have appeared more cylindrical in life. These vertebrae possess low neural arches and no transverse processes, and only possess weak zygapophyses (Figure 6a–i). Of the eight, the second in the series is the best preserved (Figure 6d–i). Dorsally it is smooth, and there are no distinct features ventrally, though this may be a factor of compaction as a distinct ventral keel is present on the ventral surface of the dorsal vertebra (Figure 6o).

3.3.2 | Ribs

Portions of ribs are preserved but are moderately fragmented and do not preserve any articulating or distal surfaces (Figure 7). Unfortunately, it is difficult to tell how many ribs these fragments represent in total.

3.3.3 | Ilium

The left ilium is the only pelvic element preserved (Figure 8). In lateral view, the anterior margin of the acetabulum is somewhat deteriorated, though it can be determined to be roughly circular, and a pronounced supraacetabular crest frames the dorsal margin of the acetabulum. More posteriorly, the dorsal margin of the acetabulum smoothly transitions into the dorsal blade and lacks any sculpturing. The dorsal blade is posteriorly directed and is similar in morphology to that of *Youngina capensis* (Gow, 1975). A sacral facet is present on the medial surface on the posterior margin of the ilium. In dorsal view, the dorsal blade is laterally compressed andpossesses no distinct features or expansions. Its maximum anteroposterior length and dorsoventral height is 7.60 and 5.75 mm, respectively. No preacetabular process is present.

3.3.4 | Zeugopodium/Stylopodium

Four fragmented elements are identified as limb bones (Figure 9), though they are quite badly compressed and preserve few distinct

FIGURE 7 Ribs from BP/1/5296 in situ.

features, hampering reliable identification. Perhaps the most identifiable bone is the ulna, as it is found semi-articulated with the ulnare (Figure 9k,l). The distal articulating surface of this bone is flat and would make a good fit with the flat articulating surface of the ulnare.

3.3.5 | Ulnare and Intermedium

A collection of small bones is found in close proximity to one another and are likely wrist bones (Figure 1). Of these bones, we identify an ulnare and intermedium (Figure 9k,l,p–s). The proximal surface of the intermedium possesses a furrowing groove that matches with that of the ulnare for the perforating artery. The ulnare is a disk-like element with thickened margins.

3.3.6 | Phalanges

Two digits are partially preserved (Figure 10). The less complete of the two is presumed to belong to the manus because of its close proximity to the ulnare, intermedium, and a series of other wrist bones. The more complete digit is thought to belong to the pes because of its proximity to the pelvic girdle and caudal vertebrae. The more complete digit (Figure 10a,b) is composed of four nearly complete and semi-articulated phalanges associated with a partial ungual phalanx. The first three phalanges decrease in size, while the penultimate phalanx is slightly longer than that of the antepenultimate phalanx (Table 2). The associated phalanx is eroded proximally, but the preserved portion shows no evidence that it was strongly recurved. The second digit (Figure 10c,d) is represented by three phalanges, the two most proximal of which are complete or nearly so. The most distal phalanx is only represented by a proximal fragment. Notably, the largest, most proximal phalanx is quite robust, compared with the more slender nature of the other phalanges present in both digits.

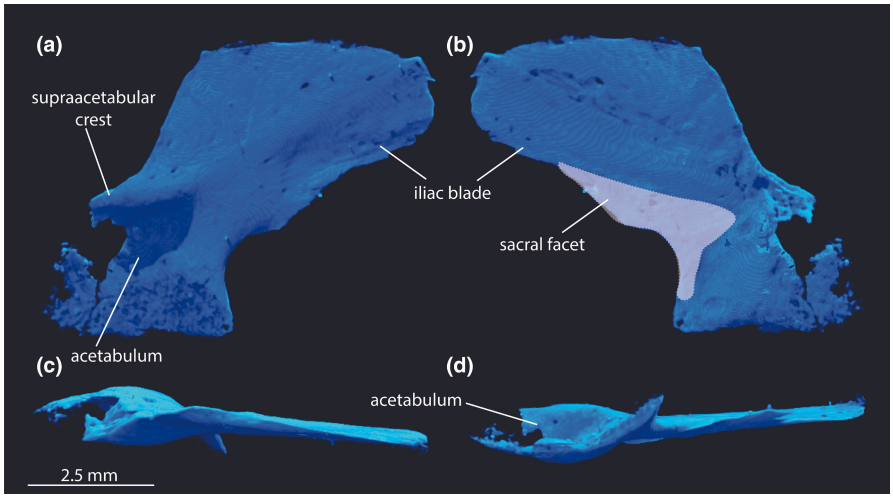

FIGURE 8 Left ilium from. BP/1/5296. (a) Lateral, (b) medial, (c) dorsal, and (d) ventral view.

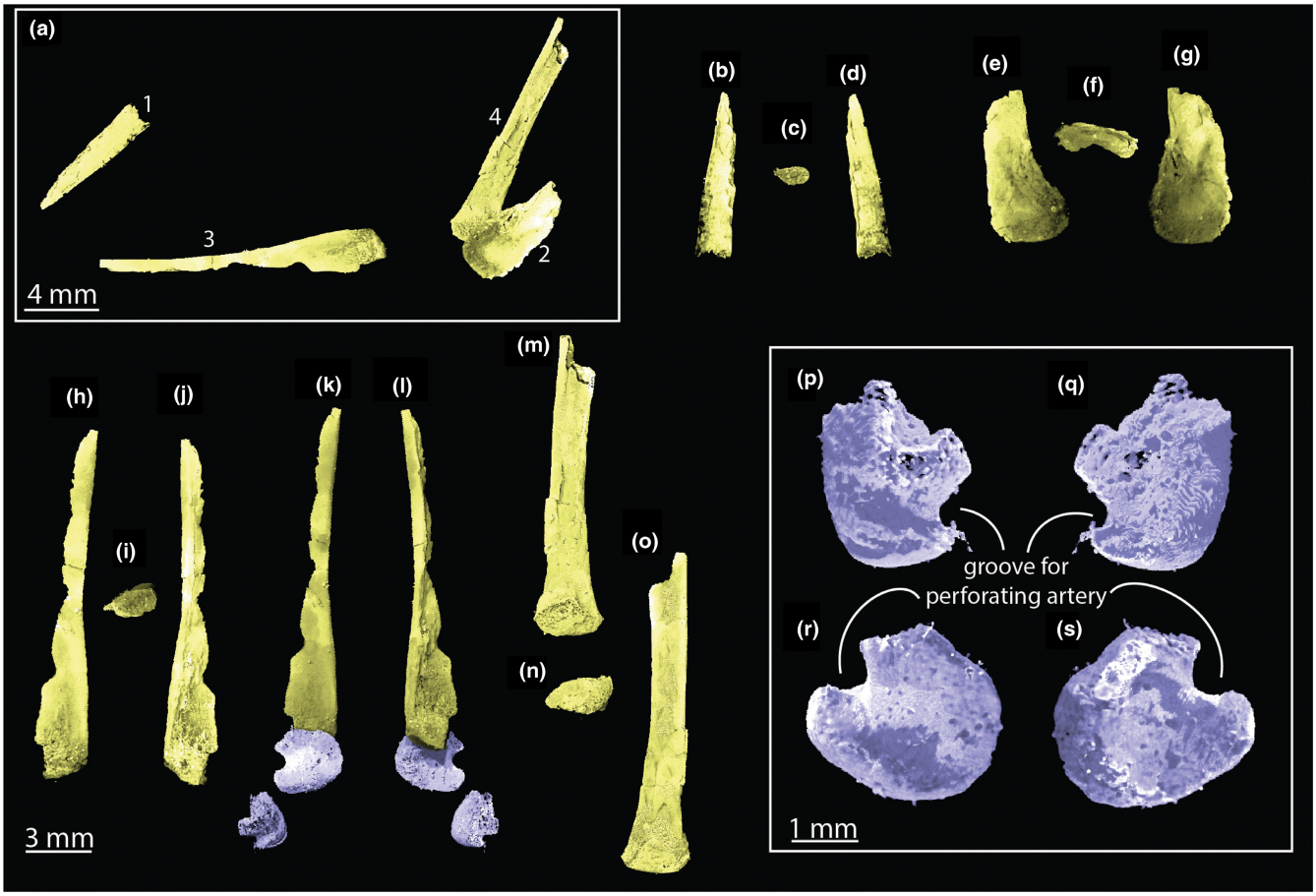

FIGURE 9 Limb bones from BP/1/5296. (a) Material in situ, (b–d) limb 1 in a, (e–g) limb 2 in a, (h–j) limb 3 (ulna) in a in (h) dorsal, (i) distal, and (j) ventral view, (k, l) limb 3 (ulna) from a with the ulnare and intermedium in situ in (k) dorsal and (l) ventral view, (m–o) limb 4 from a. Intermedium in (p) dorsal and (q) ventral view. Ulnare in (r) dorsal and (s) ventral view. While c, f, i, and n likely show the distal articulation surface, it cannot be determined which views of the long bones represent medial or lateral view.

3.4 | Phylogenetic analyses

We recover *Palacrodon* as branching immediately prior to the crown diapsid node in all parsimony analyses. Our equal weights parsimony analysis resulted in 28 most parsimonious trees (length = 1242 steps; CI = 0.304; RI = 0.641) in which the strict consensus tree generated from the optimal trees shows *Palacrodon* within a polytomy with *Thadeosaurus colcanapi*,

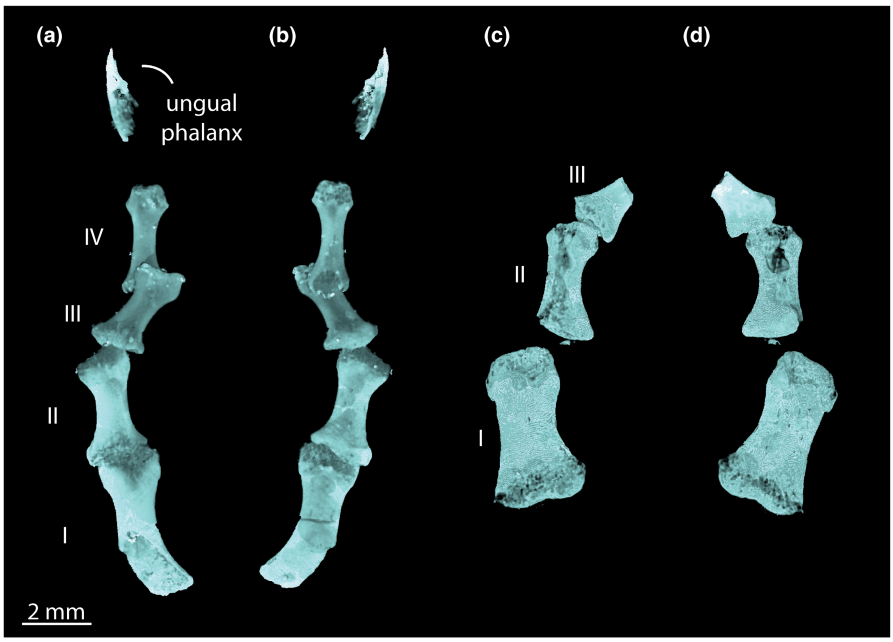

FIGURE 10 Two partial pedal digits from BP/1/5296. The first digit in (a) extensor and (b) flexor view, and the second digit in (c) extensor and (d) flexor view.

TABLE 2 Pedal digit measurements from BP/1/5296 as they appear in Figure 10. Measurements reported in millimeters.

Phalange	Proximal-distal length	Width of proximal articulation surface	Width of proximal articulation surface	Width midshaft
Figure 10a-I	4.31	–	1.73	1.15
Figure 10a-II	3.19	1.88	1.56	0.93
Figure 10a-III	2.66	1.59	1.38	0.84
Figure 10a-IV	3.36	1.20	1.04	0.67
Figure 10c-I	4.40	2.59	1.96	1.63
Figure 10c-II	3.28	–	1.64	1.11

Hovasaurus boulei, *Acerosodontosaurus piveteaui*, *Claudiosaurus germaini*, the younginids, and wiegeltisaurids, just outside of crown Diapsida. Weighted parsimony analyses also consistently recover *Palacrodon* just outside of the diapsid crown, regardless of K value, and more consistently resolve the position of *Thadeosaurus colcanapi*, *Acerosodontosaurus piveteaui*, and *Hovasaurus boulei*. Using the recommended K value of 12 (Goloboff et al., 2018), we recover *Palacrodon* outside of the crown node (Figure 11; Fit: 52.72016). In this analysis, we recover *T. colcanapi*, *A. piveteaui*, and *H. boulei* in a clade sister to *Youngina capensis*. All of these relations are maintained in the analysis using a K value of 6 (Fit: 84.66270). The analysis with K of 3 (Fit: 123.52917) recovers the same position for *Palacrodon* as well as the *T. colcanapi*, *A. piveteaui*, and *H. boulei* clade, but recovers *Y. capensis* successively stemward. The Bayesian analysis corroborates the stem position of *Palacrodon* just outside of the crown reptilian node, though it recovers *Palacrodon* in a polytomy with *Thadeosaurus colcanapi*, *Acerosodontosaurus piveteaui*, *Hovasaurus boulei*, and *Youngina capensis*, similar to the equal weights parsimony analysis.

4 | DISCUSSION

While crown reptiles, particularly archosauromorphs, experienced a major radiation during the Triassic (Brusatte et al., 2010; Ezcurra, 2016; Foth et al., 2016; Nesbitt, 2011), few stem representatives survived the Permo-Triassic mass extinction, including procolophonid parareptiles (Ruta et al., 2011), weigeltisaurids (Brinkman, 1988), tangasaurids (Ketchum & Barrett, 2004), and potentially drepanosaurs, which have been recovered both outside and within crown reptiles (Pritchard & Nesbitt, 2017). The phylogenetic placement of *Palacrodon* within the stem lineage is not only informative for understanding the success and longevity of the stem group following the Permo-Triassic mass extinction as well as Triassic ecology, but also anatomical transitions between the stem and crown group.

The bones preserved in BP/1/5296 suggest possible scansorial capabilities for *Palacrodon*. In many ways the postcranial elements preserved are unspecialized for arboreality, including the unspecialized pelvis and the ungual phalanx that lacks pronounced curvature

(Figure 12). The close proximity of the sacral facet and acetabulum seen in *Palacrodon*, with the sacral facet located at the base of the dorsal blade, is similar to that of extant iguanians capable of facultative bipedality (Borsuk-Bialynicka, 2008). Additionally, the dorsal margin of the acetabulum smoothly transitions into the dorsal blade and lacks any sculpturing, a feature said to allow the femur to be raised high during bipedal locomotion (Gow, 1975). Previous work also shows that claw morphology is linked to substrate use and habitat (Baeckens et al., 2019; D'Amore et al., 2018; Tulli et al., 2009), and the straight nature of the ungual preserved for *Palacrodon* would suggest terrestrial habits. These features would not outright suggest that *Palacrodon* regularly scaled trees.

However, it is possible that *Palacrodon* had enhanced clinging capabilities, as indicated by the longer length of the penultimate phalanx compared with that of the antepenultimate phalanx (Fröbisch & Reisz, 2009; Luo et al., 2003). This condition has evolved repeatedly in arboreal amniotes (Table 3), as seen in various mammals such as colugos, megachiropterans, and woolly opossums (Boyer & Bloch, 2008; Hamrick, 2001; Luo et al., 2003), lizards (Arnold, 1998; Fontanarrosa & Abdala, 2016; Fröbisch & Reisz, 2009), and birds (Hopson, 2001), and the presence of elongate proximal phalanges has been used to infer arboreality for many fossil taxa (Clark et al., 1998; Evans & Barbadillo, 1998; Fröbisch & Reisz, 2009; Heckert et al., 2005; Hopson, 2001; Luo et al., 2003; Wang et al., 2008). Changes in phalangeal proportions are strongly linked to substrate use and rarely occur in the absence of a locomotor shift (Arnold, 1998; Tulli et al., 2009), and the degree of elongation seen in the penultimate phalanx of *Palacrodon* suggests it was capable of occasionally climbing or clinging, thought it was likely not adeptly living in an arboreal habitat.

Though phalangeal proportions have been used to suggest arboreal capabilities, the presence of weakly recurved unguals may suggest otherwise of *Palacrodon*. However, a variety of extant reptiles, particularly lizards, are capable of climbing despite lacking recurved

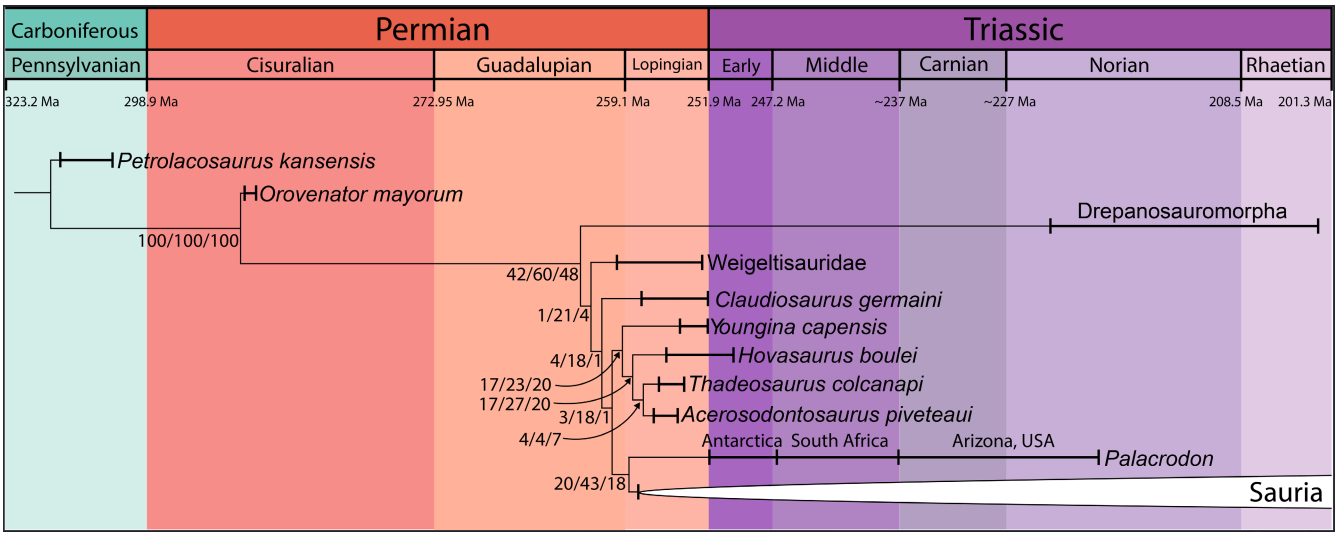

FIGURE 11 Tree resulting from weighted (K = 12) parsimony analysis. Known or estimated chronostratigraphic uncertainty of taxa are represented by bracketed bold lines and may underestimate actual stratigraphic ranges. *Palacrodon* is represented at the generic level with specimens found in Antarctica, South Africa, and Arizona, and phylogenetic coding for *Palacrodon* reflects on BP/1/5296. Values at notes are GC bootstrap (left value), absolute frequency bootstrap (middle), and symmetric (right value) support values.

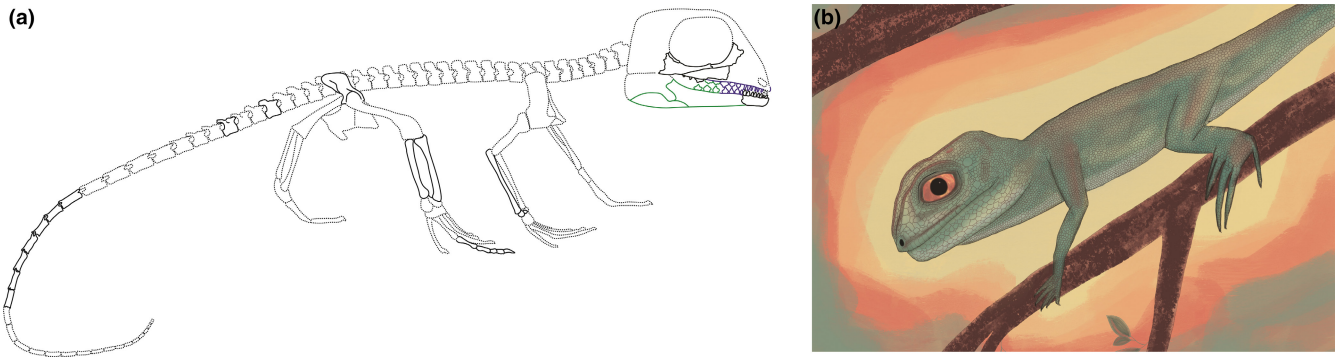

FIGURE 12 Reconstructions of *Palacrodon*. (a) *Palacrodon* composite skeleton based upon the skeletal material present (solid black outline), the fossil impression visible externally (blue), and photograph of the latex peel (green); (b) *Palacrodon* life reconstruction (illustration by K.M. Jenkins).

TABLE 3 Instances of elongation of the penultimate phalanx and claw recurvature in extant and fossil examples, as compared with closely related sister-taxa.

Taxon	Penultimate phalanx longer than antepenultimate	Recurved claws	Ecology or inferred ecology	Source	Sister-taxon	Penultimate phalanx longer than antepenultimate	Recurved claws	Ecology or inferred ecology	Source
Scelarcis oxycephala	Yes	Yes	Rock climbing	Arnold (1998)	*Acanthodactylus erythrurus*	No	No	Terrestrial	Arnold (1998)
Scelarcis perspicillata	Yes	Yes	Rock climbing	Arnold (1998)					
Holaspis guentheri	Yes	Yes	Arboreal	Arnold (1998)					
Anolis cuvieri	Yes	Yes	Arboreal	Tulli et al. (2009), UMMZ 73635	*Anolis humilis*	No	No	Terrestrial	Tulli et al. (2009), MCZ 177846
Anolis gundlachi	Yes	Yes	Arboreal	Tulli et al. (2009), UF 85085					
Anolis limifrons	Yes	Yes	Arboreal	Tulli et al. (2009), UF 31201					
Scandensis ciervensis†	Yes	Yes	Arboreal	Evans and Barbadillo (1998)	*Bavarisaurus macrodactylus*†	No	No	Terrestrial	Evans (1994)
Trilophosaurus buettneri†	Yes	Yea	Arboreal	Heckert et al. (2005)	*Azendohsaurus madagaskarensis*†	No	Yes	Terrestrial	Nesbitt (2011)
Weigeltisaurus jaekeli†	Yes	Yes	Arboreal	Pritchard et al. (2021)	*Claudiosaurus germaini*†	No	No	Aquatic	Carroll (1981)
					Thadeosaurus colcanapi†	Yes/No	No	Aquatic	Carroll (1981)
					Hovasaurus boulei†	No	No	Aquatic	Currie (1981)
Suminia getmanovi†	Yes	Yes	Arboreal	Fröbisch and Reisz (2009)	*Galechirus scholtzi*†	No	No	Terrestrial	Brinkman (1988)

Note: Specimens referenced provided by https://www.morphosource.org/. Daggers (†) indicate extinct taxa.Abbreviations: MCZ—Museum of Comparative Zoology, Harvard University, Cambridge, Massachusetts, United States; UF—Florida Museum, University of Florida, Gainesville, Florida, United States.

claws. Particularly, the trunk-ground ecomorph associated with the *Anolis* adaptive radiation possesses distinctly less recurved claws than the fully arboreal ecomorphs, though it is capable of occasionally scaling trees (Yuan et al., 2018). Even the reduction and complete loss of claws is seen in some geckos whose climbing abilities are enhanced by gripping toepads and digital lamellae (Khannoon et al., 2015; Russell & Bauer, 2008). We cannot confirm the presence of such soft tissue structures in *Palacrodon*, just as we cannot assert a fully arboreal lifestyle for this taxon. But, we assert that the presence of elongated phalanges is indicative of some locomotor shift, potentially the ability to occasionally climb vegetation. Frequently, an organism's performance in and interaction with its environment relies on the composite of its phenotype, and less so on the phenotype of a singular trait, such as claw curvature (Yuan et al., 2018). Coupled with the characteristically herbivorous dentition found in *Palacrodon*, these traits suggest some regular interaction with vegetation.

Few known vertebrates explored arboreal habitats during the Paleozoic (Evans & Haubold, 1987; Fröbisch & Reisz, 2009; Mann et al., 2021; Spindler et al., 2018), while there is widespread evidence of arboreality by the Late Triassic (Figure 13) (Ezcurra et al., 2020; Heckert et al., 2005; Renesto et al., 2010; Stein et al., 2008). Widespread arboreality seems to be limited to the latter phases of the Triassic, as there are few examples of arboreal or even scansorial taxa from the earlier phases of the Triassic. Not only did the end-Permian mass extinction eliminate numerous animal lineages, but it devastated plant life as well, with a preferential loss of vegetation capable of sustaining arboreal vertebrates (e.g., conifers, lycopsids), which did not fully recover until the Middle to Late Triassic (Grauvogel-Stamm & Ash, 2005; Looy et al., 2001; Visscher et al., 2011). This loss of trees may have contributed to the extinction of late Permian arboreal vertebrates, including grasping anomodonts (Fröbisch & Reisz, 2009) and gliding weigeltisaurids (Evans & Haubold, 1987; Pritchard et al., 2021). The subsequent return of arboreal ecosystems in the Late Triassic reestablished niche space that drepanosaurs, trilophosaurs, kuehneosaurs, and pterosaurs occupied (Bennett, 1997; Heckert et al., 2005; Evans & Jones, 2010; Renesto et al., 2010; potentially also lagerpetids, see Ezcurra et al., 2020). The presence of manual anatomy congruent with the grasping ability necessary for a climbing habitus and potentially scansorial semi-arboreal lifestyle in *Palacrodon*, combined with dentition that is suited toward griding plant material (Gow, 1992; Jones, 2009; Sues & Baird, 1998), indicates the presence of some vegetation in the earliest phases of the Triassic. It also shows that plant recovery was possibly enabling the reptile clades that persisted into the Triassic to begin to fulfill new ecologic roles (Singh et al., 2021).

4.1 | *Palacrodon* illustrates an intermediate stapedial morphology

Stapedial morphology changes drastically during the transition from early tetrapods to that of crown reptiles (Figure 14). Stem

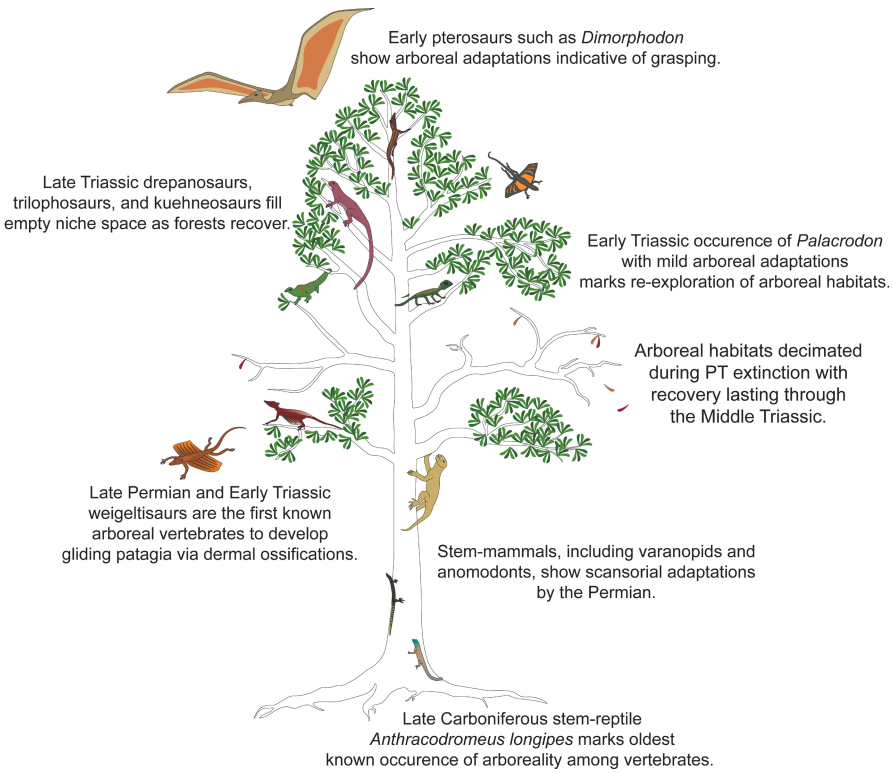

FIGURE 13 Early instances of arboreality among amniotes and the reentry into arboreal niche space following the end-Permian extinction. Diagram is to be read from the bottom toward the top as if progressing on a timeline spanning the Late Carboniferous to the Late Triassic.

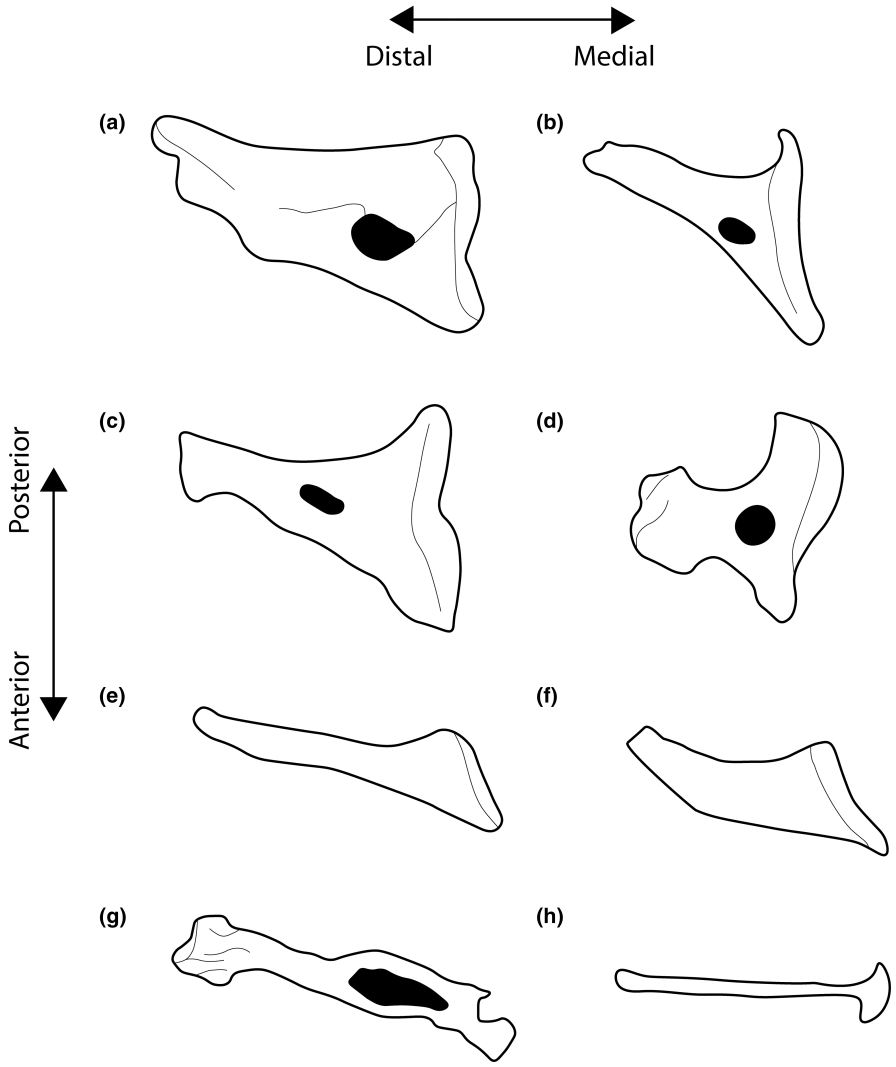

FIGURE 14 Stapes from early tetrapods and stem and crown reptiles. Stapedial morphology of an early tetrapod (a), stem reptiles (b–g), and crown reptiles (h). (a) *Acanthostega gunnari* modified from (Clack et al., 2016), (b) *Euconcordia cunninghami* (original), (c) *Orovenator mayorum* modified from (Ford & Benson, 2019), (d) *Australothyris smithi* modified from (Modesto et al., 2009), (e) BP/1/5296 (original), (f) *Avicranium renestoi* (original), (g) *Youngina capensis* modified from (Gardner et al., 2010), (h) *Crocodylus* sp.(original). Morphology of *Crocodylus* is similar to that of testudines and Lepidosauria. All stapes are in ventral view. Objects are not to scale.

and crown reptiles are described as having either robust or slender stapes, indicative respectively of low- and high-frequency hearing (Clack, 2002; Clack et al., 2016). This is often discussed in a binary context in combination with a presence-absence concept of a tympanic membrane based on quadrate emargination or the presence of an otic notch (Sobral et al., 2016). The stapes of *Palacrodon* (Figure 14e) lack the structural robusticity seen in early tetrapods and stem reptiles, but it is not as slender as the stapes of taxa known or inferred to have impedance-matching ears (Figure 14h). The columella is slightly flattened like most stem reptiles and early tetrapods, but it approaches the more rod-like and elongate morphology of crown reptiles. As it is found in weak articulation with a fragment of the quadrate (Figure 4k,l), it is unlikely that *Palacrodon* possessed a tympanic membrane. Its weak articulation compared with earlier stem reptiles, such as the captorhinid *Euconcordia cunninghami* and the diapsid *Orovenator mayorum* (Figure 14b,c), may indicate some free movement of the stapes (Müller et al., 2018; Sobral et al., 2016). Though not capable of transmitting high frequency sounds like crown reptiles, the morphology of the stapes therefore suggests the ability to transmit sounds of a higher frequency than that of earlier taxa. Similar hearing capabilities were suggested for *Youngina capensis* (Gardner et al., 2010; Walsh et al., 2013), though its stapes is considerably more elongate than that of *Palacrodon*.

Transitions in hearing have been discussed to some extent within parareptiles (Müller et al., 2018; Müller & Tsuji, 2007), but the sequence of events that occurred during the independent acquisition of impedance-matching in crown reptiles is still ambiguous. Competing hypotheses exist for the evolution of high-frequency (tympanic) hearing among crown reptiles: (1) it is ancestral to crown reptiles, or (2) it arose independently in Lepidosauria, Archosauria, and Testudines (Clack, 1997; Müller et al., 2018; Sobral et al., 2016).

Some recent work favors the second and argues that the shallow quadrate emargination of stem-saurian *Youngina capensis* would not have supported a tympanic membrane, thus suggesting a lack of tympanic hearing at the base of the crown (Gardner et al., 2010; Müller et al., 2018; Sobral et al., 2016). Furthermore, the somewhat robust but columnar stapes of the stem-turtle *Proganochelys quenstedti* would not have been impedance-matching (Gaffney, 1990; Lautenschlager et al., 2018). The stapes associated with *Palacrodon* here, *Y. capensis*, early crown reptiles such as *P. quenstedti*, along with our inferred phylogenetic position of *Palacrodon*, implies an intermediate state of hearing capabilities and a gradual transition from low frequency to high frequency in the late Permian and Early Triassic. We posit that stapedial evolution was more gradual than previously hypothesized, and middle ear specializations for higher-frequency hearing preceded external ear (tympano-quadrate) specializations.

5 | CONCLUSIONS

The Antarctic specimen of *Palacrodon* reveals the taxon's phylogenetic placement as a near-crown stem reptile and preserves anatomical features that support the presence of some robust vegetation during the end-Permian mass extinction recovery phase. The presence of a moderately robust stapes in articulation with a fragment of the quadrate in the studied specimen supports the notion of an intermediate phase of hearing within the reptilian lineage and the hypothesis that middle ear specializations preceded that of the external ear. Further faunal analyses of Early Triassic tetrapods have the potential to untangle the complex evolutionary origins of crown reptiles, and the success of the stem group following the Permo–Triassic boundary.

AUTHOR CONTRIBUTIONS

K.M.J. initiated project. J.N.C. provided CT scan, and K.M.J. segmented scan. K.M.J. and D.M. scored characters and conducted phylogenetic analyses. K.M.J. produced illustrations, photos, and figures. All authors contributed to the writing and editing of the manuscript.

The authors declare no conflict of interest.

ACKNOWLEDGMENTS

We thank P.J. Hancox, J.A. Gauthier, and A. Fitch for helpful discussions that greatly improved this work. Helpful reviews that improved the quality of this manuscript were provided by Martín Ezcurra. A. Ruebenstahl provided helpful advice regarding parsimony analyses, and G. Chinamatira scanned the specimen. Financial support was provided by Department of Earth and Planetary Sciences, Yale University, Sigma Xi National Science Foundation grant 2046868, NRF African Origins Platform grant 98800, and Sigma Xi GIAR.

DATA AVAILABILITY STATEMENT

CT data and 3D meshes are available on Morphosource.org.

ORCID

Kelsey M. Jenkins https://orcid.org/0000-0002-6345-6553
Dalton L. Meyer https://orcid.org/0000-0003-0050-6354

REFERENCES

Arnold, E. (1998) Structural niche, limb morphology and locomotion in lacertid lizards (Squamata, Lacertidae); a preliminary survey. *Bulletin of the Natural History Museum of London*, 64, 63–90.

Baeckens, S., Goeyers, C. & Van Damme, R. (2019) Convergent evolution of claw shape in a transcontinental lizard radiation. *Integrative and Comparative Biology*, 60, 10–23.

Bennett, S.C. (1997) The arboreal leaping theory of the origin of pterosaur flight. *Historical Biology*, 12, 265–290.

Borsuk-Bialynicka, M. (2008) Evolution of the iliosacral joint in diapsid phylogeny. *Neues Jahrbuch für Geologie und Paläontologie-Abhandlungen*, 249, 297–311.

Botha, J. & Smith, R.M. (2006) Rapid vertebrate recuperation in the Karoo Basin of South Africa following the end-Permian extinction. *Journal of Earth Sciences*, 45, 502–514.

Boyer, D.M. & Bloch, J.I. (2008) Evaluating the mitten-gliding hypothesis for Paromomyidae and Micromomyidae (Mammalia, "Plesiadapiformes") using comparative functional morphology of new Paleogene skeletons. In: Sargis, E.J. & Dagosto, M. (Eds.) *Mammalian evolutionary morphology: a tribute to Frederick S. Szalay*. The Netherlands: Springer, pp. 233–284.

Brinkman, D. (1988) A weigeltisaurid reptile from the lower Triassic of British Columbia. *Palaeontology*, 31, 951–956.

Broom, R. (1906) On a new south African Triassic rhynchocephalian. *Transactions of the South African Philosophical Society*, 16, 21–23.

Brusatte, S.L., Benton, M.J., Lloyd, G.T., Ruta, M. & Wang, S.C. (2010) Macroevolutionary patterns in the evolutionary radiation of archosaurs (Tetrapoda: Diapsida). *Earth and Environmental Science Transactions of the Royal Society of Edinburgh*, 101, 367–382.

Carroll, R.L. (1981) Plesiosaur ancestors from the upper Permian of Madagascar. *Philosophical Transactions of the Royal Society of London, B*, 1066, 315–383.

Clack, J.A. (1997) The evolution of tetrapod ears and the fossil record. *Brain, Behavior and Evolution*, 50, 198–212.

Clack, J.A. (2002) Patterns and processes in the early evolution of the tetrapod ear. *Journal of Neurobiology*, 53, 251–264.

Clack, J.A., Fay, R.R. & Popper, A.N. (2016) *Evolution of the vertebrate ear: evidence from the fossil record*. New York: Springer, p. 355.

Clark, J., Hopson, J., Fastovsky, D. & Montellano, M. (1998) Foot posture in a primitive pterosaur. *Nature*, 391, 886–889.

Collinson, J.W., Hammer, W.R., Askin, R.A. & Elliot, D.H. (2006) Permian-Triassic boundary in the central Transantarctic Mountains, Antarctica. *Geological Society of America Bulletin*, 118, 747–763.

Currie, P.J. (1981) *Hovasaurus boulei*, an aquatic eosuchian from the Upper Permian of Madagascar. *Palaeontologia Africana*, 24, 99–168.

D'Amore, D.C., Clulow, S., Doody, J.S., Rhind, D. & McHenry, C.R. (2018) Claw morphometrics in monitor lizards: variable substrate and habitat use correlate to shape diversity within a predator guild. *Ecology and Evolution*, 8, 6766–6778.

Evans, S.E. (1994) The Solnhofen (Jurassic: Tithonian) lizard genus Bavarisaurus: new Skull material and a reinterpretation. *Neues Jahrbuch für Geologie und Paläontologie Abhandlungen*, 192, 37–52.

Evans, S. & Barbadillo, L. (1998) An unusual lizard (Reptilia: Squamata) from the early cretaceous of las Hoyas, Spain. *Zoological Journal of the Linnean Society*, 124, 235–265.

Evans, S. & Haubold, H. (1987) A review of the upper Permian genera *Coelurosauravus*, *Weigeltisaurus* and *Gracilisaurus* (Reptilia: Diapsida). *Zoological Journal of the Linnean Society*, 90, 275–303.

Evans, S. & Jones, M.E. (2010) The origin, early history and diversification of lepidosauromorph reptiles. In: Bandyopadhyay, S. (Ed.) *New aspects of Mesozoic biodiversity*. Berlin: Springer, pp. 27–44.

Ezcurra, M.D. (2016) The phylogenetic relationships of basal archosauromorphs, with an emphasis on the systematics of proterosuchian archosauriforms. *PeerJ*, 4, e1778.

Ezcurra, M.D. & Butler, R.J. (2018) The rise of the ruling reptiles and ecosystem recovery from the Permo-Triassic mass extinction. *Proceedings of the Royal Society B*, 285, 20180361.

Ezcurra, M.D., Nesbitt, S.J., Bronzati, M., Dalla Vecchia, F.M., Agnolin, F.L., Benson, R.B. et al. (2020) Enigmatic dinosaur precursors bridge the gap to the origin of Pterosauria. *Nature*, 588, 445–449.

Fontanarrosa, G. & Abdala, V. (2016) Bone indicators of grasping hands in lizards. *PeerJ*, 4, e1978.

Ford, D.P. & Benson, R.B. (2019) A redescription of *Orovenator mayorum* (Sauropsida, Diapsida) using high-resolution μCT, and the consequences for early amniote phylogeny. *Papers in Palaeontology*, 5, 197–239.

Foth, C., Ezcurra, M.D., Sookias, R.B., Brusatte, S.L. & Butler, R.J. (2016) Unappreciated diversification of stem archosaurs during the middle Triassic predated the dominance of dinosaurs. *BMC Evolutionary Biology*, 16, 1–10.

Fröbisch, J. & Reisz, R.R. (2009) The late Permian herbivore *Suminia* and the evolution of arboreality in terrestrial vertebrate ecosystems. *Proceedings of the Royal Society B*, 276, 3611–3618.

Gaffney, E.S. (1990) The comparative osteology of the Triassic turtle *Proganochelys*. *Bulletin of the American Museum of Natural History*, 194, 1–268.

Gardner, N.M., Holliday, C.M. & O'Keefe, F.R. (2010) The braincase of *Youngina capensis* (Reptilia, Diapsida): new insights from high-resolution CT scanning of the holotype. *Palaeontologia Electronica*, 13, 1–16.

Gauthier, J.A., Estes, R. & de Queiroz, K. (1988) A phylogenetic analysis of the Lepidosauromorpha. In: Estes, R. & Pregill, G. (Eds.) *Phylogenetic relationships of the lizard families: essays commemorating Charles L. camp*. Stanford: Stanford University Press, pp. 15–98.

Goloboff, P.A. & Catalano, S.A. (2016) TNT version 1.5, including full implementation of phylogenetic morphometrics. *Cladistics*, 32, 221–238.

Goloboff, P.A., Torres, A. & Arias, J.S. (2018) Weighted parsimony outperforms other methods of phylogenetic inference under models appropriate for morphology. *Cladistics*, 34, 407–437.

Gow, C.E. (1975) The morphology of relationships of *Youngina capensis* Broom and *Prolacerta broomi* Parrington. *Palaeontologica Africana*, 18, 89–131.

Gow, C.E. (1992) An enigmatic new reptile from the lower Triassic Fremouw formation of Antarctica. *Palaeontologica Africana*, 29, 21–23.

Gow, C.E. (1999) The Triassic reptile *Palacrodon browni* Broom, synonymy and a new specimen. *Palaeontologica Africana*, 35, 21–23.

Grauvogel-Stamm, L. & Ash, S.R. (2005) Recovery of the Triassic land flora from the end-Permian life crisis. *Comptes Rendus Palevol*, 4, 593–608.

Hamrick, M.W. (2001) Primate origins: evolutionary change in digital ray patterning and segmentation. *Journal of Human Evolution*, 40, 339–351.

Hancox, P., Damiani, R. & Hammer, W.R. (2020) Biostratigraphy of the *Cynognathus* assemblage zone (Beaufort group, Karoo supergroup), South Africa. *South African Journal of Geology*, 123, 217–238.

Heaton, M.J. (1979) Cranial anatomy of primitive captorhinid reptiles from the late Pennsylvanian and early Permian, Oklahoma and Texas. *Bulletin of the Oklahoma Geological Survey*, 127, 1–84.

Heckert, A.B., Spielmann, J.A. & Lucas, S.G. (2005) The late Triassic archosauromorph *Trilophosaurus* as an arboreal climber. *Rivista Italiana di Paleontologia e Stratigrafia*, 111, 395–412.

Hopson, J.A. (2001) Ecomorphology of avian and nonavian theropod phalangeal proportions: implications for the arboreal versus terrestrial origin of bird flight. In: Gauthier, J. & Gall, L. (Eds.) *New perspectives on the origin and early evolution of birds: proceedings of the international symposium in honor of John Ostrom*. New Haven: Peabody Museum of Natural History, pp. 211–235.

Huelsenbeck, J.P. & Ronquist, R. (2001) MRBAYES: Bayesian inference of phylogenetic trees. *Bioinformatics*, 17, 754–755.

Jones, M. (2009) Dentary tooth shape in *Sphenodon* and its fossil relatives (Diapsida: Lepidosauria: Rhynchocephalia). *Fronteirs in Oral Biology*, 13, 9–15.

Ketchum, H.F. & Barrett, P.M. (2004) New reptile material from the lower Triassic of Madagascar: implications for the Permian Triassic extinction event. *Canadian Journal of Earth Sciences*, 41, 1–8.

Khannoon, E.R., Russell, A.P. & Tucker, A.S. (2015) Developmental mechanisms underlying differential claw expression in the autopodia of geckos. *EvoDevo*, 6, 8.

Kitching, J.W., Collinson, J.W., Elliot, D.H. & Colbert, E.H. (1972) *Lystrosaurus* zone (Triassic) fauna from Antarctica. *Science*, 175, 524–527.

Kligman, B., Marsh, A.D. & Parker, W.G. (2018) First records of diapsid *Palacrodon* from the Norian, late Triassic Chinle formation of Arizona, and their biogeographic implications. *Acta Palaeontologica Polonica*, 63, 117–127.

Lautenschlager, S., Ferreira, G.S. & Werneburg, I. (2018) Sensory evolution and ecology of early turtles revealed by digital endocranial reconstructions. *Frontiers in Ecology and Evolution*, 6, 1–7.

Lewis, P.O. (2001) A likelihood approach to estimating phylogeny from discrete morphological character data. *Systematic Biology*, 6, 913–925.

Looy, C.V., Twitchett, R.J., Dilcher, D.L., Van Konijnenburg-Van Cittert, J.H.A. & Visscher, H. (2001) Life in the end-Permian dead zone. *Proceedings of the National Academy of Sciences*, 98, 7879–7883.

Luo, Z.-X., Ji, Q., Wible, J.R. & Yuan, C.-X. (2003) An early cretaceous tribosphenic mammal and metatherian evolution. *Science*, 302, 1934–1940.

Mann, A., Dudgeon, T.W., Henrici, A.C., Berman, D.S. & Pierce, S.E. (2021) Digit and ungual morphology suggest adaptations for scansoriality in the late carboniferous eureptile *Anthracodromeus longiceps*. *Frontiers in Earth Science*, 9, 675337.

McManus, H.A., Taylor, T.N. & Collinson, J.W. (2002) A petrified *glossopteris* flora from Collinson ridge, central Transantarctic Mountains: late Permian or early Triassic? *Review of Palaeobotany and Palynology*, 120, 233–246.

Modesto, S.P., Scott, D.M. & Reisz, R.R. (2009) A new parareptile with temporal fenestration from the middle Permian of South Africa. *Canadian Journal of Earth Sciences*, 46, 9–20.

Müller, J. & Tsuji, L.A. (2007) Impedance-matching hearing in Paleozoic reptiles: evidence of advanced sensory perception at an early stage of amniote evolution. *PLoS One*, 9, e889.

Müller, J., Bickelmann, C. & Sobral, G. (2018) The evolution and fossil history of sensory perception in amniote vertebrates. *Annual Review of Earth and Planetary Sciences*, 46, 495–519.

Nesbitt, S.J. (2011) The early evolution of Archosauria: relationships and the origin of major clades. *Bulletin of the American Museum of Natural History*, 352, 1–292.

Neveling, J. (2004) Stratigraphic and sedimentological investigation of the contact between the *lystrosaurus* and the *Cynognathus* assemblage zones (Beaufort group: Karoo supergroup). *Council for Geoscience Bulletin*, 137, 1–141.

Peecook, B.R., Smith, R.M. & Sidor, C.A. (2018) A novel archosauromorph from Antarctica and an updated review of a high-latitude vertebrate assemblage in the wake of the end-Permian mass extinction. *Journal of Vertebrate Paleontology*, 38, e1536664.

Pritchard, A.C. & Nesbitt, S.J. (2017) A bird-like skull in a Triassic diapsid reptile increases heterogeneity of the morphological and phylogenetic radiation of Diapsida. *Royal Society Open Science*, 4, 170499.

Pritchard, A.C. & Sues, H.-D. (2019) Postcranial remains of *Teraterpeton hrynewichorum* (Reptilia: Archosauromorpha) and the mosaic evolution of the saurian postcranial skeleton. *Journal of Systematic Palaeontology*, 17, 1745–1765.

Pritchard, A.C., Gauthier, J.A., Hanson, M., Bever, G.S. & Bhullar, B.-A.S. (2018) A tiny Triassic saurian from Connecticut and the early evolution of the diapsid feeding apparatus. *Nature Communications*, 9, 1–10.

Pritchard, A.C., Sues, H.-D., Scott, D. & Reisz, R.R. (2021) Osteology, relationships and functional morphology of *Weigeltisaurus jaekeli* (Diapsida, Weigeltisauridae) based on a complete skeleton from the upper Permian Kupferschiefer of Germany. *PeerJ*, 9, e11413.

Pusch, L.C., Kammerer, C.F. & Fröbisch, J. (2021) Cranial anatomy of *Bolotridon frerensis*, an enigmatic cynodont from the middle Triassic of South Africa, and its phylogenetic significance. *PeerJ*, 9, e11542.

Renesto, S., Spielmann, J.A., Lucas, S.G. & Spagnoli, G.T. (2010) The taxonomy and paleobiology of the late Triassic (Carnian-Norian: Adamanian-Apachean) drepanosaurs (Diapsida: Archosauromorpha: Drepanosauromorpha). *Bulletin of the New Mexico Museum of Natural History and Science*, 46, 1–81.

Romano, M., Bernardi, M., Petti, F.M., Rubidge, B., Hancox, J. & Benton, M.J. (2020) Early Triassic terrestrial tetrapod fauna: a review. *Earth-Science Reviews*, 103331, 103331.

Russell, A.P. & Bauer, A. (2008) The appendicular locomotor apparatus of *Sphenodon* and normal-limbed squamates. In: Gans, C., Gaunt, A. & Adler, K. (Eds.) *Biology of the Reptilia*. Ithaca: Society for the Study of Amphibians and Reptiles, pp. 1–466.

Ruta, M., Cisneros, J.C., Liebrecht, T., Tsuji, L.A. & Müller, J. (2011) Amniotes through major biological crises: faunal turnover among parareptiles and the end-Permian mass extinction. *Palaeontology*, 54, 1117–1137.

Scheyer, T.M., Spiekman, S.N.F., Sues, H.-D., Ezcurra, M.D., Butler, R.J. & Jones, M.E.H. (2020) *Colobops*: a juvenile rhynchocephalian reptile (Lepidosauromorpha), not a diminutive archosauromorph with an unusually strong bite. *Royal Society Open Science*, 7, 192179.

Sidor, C.A., Damiani, R. & Hammer, W.R. (2008) A new Triassic temnospondyl from Antarctica and a review of Fremouw formation biostratigraphy. *Journal of Vertebrate Paleontology*, 28, 656–663.

Singh, S.A., Elsler, A., Stubbs, T.L., Bond, R., Rayfield, E.J. & Benton, M.J. (2021) Niche partitioning shaped herbivore macroevolution through the early Mesozoic. *Nature Communications*, 12, 1–13.

Smith, N.D., Crandall, J.R., Hellert, S.M., Hammer, W.R. & Makovicky, P.J. (2011) Anatomy and affinities of large archosauromorphs from the lower Fremouw formation (early Triassic) of Antarctica. *Journal of Vertebrate Paleontology*, 31, 784–797.

Sobral, G., Reisz, R., Neenan, J.M., Müller, J. & Scheyer, T.M. (2016) Basal reptilians, marine diapsids, and turtles: the flowering of reptile diversity. In: Clack, J.A., Fay, R.R. & Popper, A.N. (Eds.) *Evolution of the vertebrate ear*. New York: Springer, pp. 207–243.

Spiekman, S.N. (2018) A new specimen of *Prolacerta broomi* from the lower Fremouw formation (early Triassic) of Antarctica, its biogeographical implications and a taxonomic revision. *Scientific Reports*, 8, 1–21.

Spindler, F., Werneburg, R., Schneider, J.W., Luthardt, L., Annacker, V. & Rößler, R. (2018) First arboreal 'pelycosaurs' (Synapsida: Varanopidae) from the early Permian Chemnitz fossil Lagerstätte, SE Germany, with a review of varanopid phylogeny. *PalZ*, 92, 315–364.

Stein, K., Palmer, C., Gill, P.G. & Benton, M.J. (2008) The aerodynamics of the British late Triassic Kuehneosauridae. *Palaeontology*, 51, 967–981.

Sues, H.-D. & Baird, D. (1998) Procolophonidae (Reptilia: Parareptilia) from the upper Triassic Wolfville formation of Nova Scotia, Canada. *Journal of Vertebrate Paleontology*, 18, 525–532.

Tulli, M.J., Cruz, F.B., Herrel, A., Vanhooydonck, B. & Abdala, V. (2009) The interplay between claw morphology and microhabitat use in neotropical iguanian lizards. *Zoology*, 112, 379–392.

Visscher, H., Sephton, M.A. & Looy, C.V. (2011) Fungal virulence at the time of the end-Permian biosphere crisis? *Geology*, 39, 883–886.

Walsh, S.A., Luo, Z.-X. & Barrett, P.M. (2013) Modern imaging techniques as a window to prehistoric auditory worlds. In: Köppl, C., Manley, G.A., Popper, A.N. & Fay, R.R. (Eds.) *Insights from comparative hearing research*. New York: Springer, pp. 227–261.

Wang, X., Kellner, A.W., Zhou, Z. & de Almeida Campos, D. (2008) Discovery of a rare arboreal forest-dwelling flying reptile (Pterosauria, Pterodactyloidea) from China. *Proceedings of the National Academy of Sciences*, 105, 1983–1987.

Yuan, M.L., Wake, M.H. & Wang, I.J. (2018) Phenotypic integration between claw and toepad traits promotes microhabitat specialization in the *Anolis* adaptive radiation. *Evolution*, 73, 231–244.

SUPPORTING INFORMATION

Additional supporting information can be found online in the Supporting Information section at the end of this article.

How to cite this article: Jenkins, K.M., Meyer, D.L., Lewis, P.J., Choiniere, J.N. & Bhullar, B-A. (2022) Re-description of the early Triassic diapsid *Palacrodon* from the lower Fremouw formation of Antarctica. *Journal of Anatomy*, 241, 1441–1458. Available from: https://doi.org/10.1111/joa.13770